Journal of Solid State Chemistry 236 (2016) 222–229

Contents lists available at ScienceDirect

Journal of Solid State Chemistry

journal homepage: www.elsevier.com/locate/jssc

Synthesis, crystal growth, structural and magnetic characterization of $NH_4MCl_2(HCOO)$, M=(Fe, Co, Ni)

Joshua T. Greenfield [a], V. Ovidiu Garlea [b], Saeed Kamali [c], Michael Chen [a], Kirill Kovnir [a,*]

[a] Department of Chemistry, University of California, Davis, One Shields Avenue, Davis, CA 95616, United States
[b] Quantum Condensed Matter Division, Oak Ridge National Laboratory, Oak Ridge, TN 37831, United States
[c] Mechanical, Aerospace & Biomedical Engineering Department, University of Tennessee Space Institute, Tullahoma, TN 37388, United States

ARTICLE INFO

Article history:
Received 20 July 2015
Received in revised form
16 September 2015
Accepted 16 September 2015
Available online 24 September 2015

Keywords:
Solvothermal synthesis
Crystal growth
Low-dimensional magnetism
Neutron diffraction
Mössbauer spectroscopy
Magnetic structure

ABSTRACT

An ambient-pressure solution route and an improved solvothermal synthetic method have been developed to produce polycrystalline powders and large single crystals of $NH_4MCl_2(HCOO)$ (M=Fe, Co, Ni). The magnetic structure of the 1D linear chain compound $NH_4FeCl_2(HCOO)$ has been determined by low-temperature neutron powder diffraction, revealing ferromagnetic intra-chain interactions and antiferromagnetic inter-chain interactions. The newly-reported Co and Ni analogs are isostructural with $NH_4FeCl_2(HCOO)$, but there are significant differences in the magnetic properties of each compound; the Ni analog behaves similarly to the Fe compound but with stronger magnetic coupling, exhibiting antiferromagnetic ordering (T_N=8.5 K) and a broad metamagnetic transition between 2 and 5 T, while the Co analog does not order magnetically above 2 K, despite strong antiferromagnetic nearest-neighbor interactions.

© 2015 Elsevier Inc. All rights reserved.

1. Introduction

In the field of solid-state chemistry, the accurate determination of the structure and properties of a novel compound often relies on the ability to grow a high-quality single crystal for diffraction studies and other methods of characterization. It has long been established that solvothermal syntheses, in which a reaction mixture is heated above the boiling temperature of the solvent in a closed vessel, are extremely useful for dissolving a wide variety of otherwise insoluble compounds and allowing for the controlled growth of large single crystals suitable for properties measurements [1]. One class of compounds for which this methodology is particularly well-suited is the range of transition metal (II) formates, which can form a variety of structures ranging from mesoporous 3D frameworks [2,3] to isolated 1D chains [4]. As these structures are usually composed of M^{2+} octahedra linked by various 1- or 3-atom bridging ligands [5], they often exhibit rather exotic magnetic interactions and are of interest as low-dimensional, highly anisotropic magnetic materials [6] and potentially as multiferroics [7]. We recently reported a simple solvothermal synthesis of $NH_4FeCl_2(HCOO)$, a compound composed of 1D iron–chloride–formate chains with anisotropic magnetic properties that undergoes antiferromagnetic ordering at 6 K and exhibits metamagnetic transitions in fields of 0.85–3 T, though we were not able to unambiguously determine the magnetic structure [8]. We have since performed additional characterization of the magnetic properties and have expanded our investigation to include other transition metals in the 2+ oxidation state; presented here is the magnetic structure of the prototype compound as determined by low-temperature neutron powder diffraction, as well as the synthesis, structure, and magnetic properties of the Co and Ni analogs.

2. Materials and methods

2.1. Synthesis

Warning: solvothermal reactions between transition metal chlorides and formic acid are capable of generating extremely high pressures due to the formation of various gaseous species. To minimize the risk of an explosion, reactions must be performed in suitable high-strength vessels and the concentration of formic acid should be kept as low as possible.

Phase-pure samples of $NH_4MCl_2(HCOO)$ (M=Fe, Co, Ni) were prepared by both solvothermal and ambient-pressure solution syntheses, following a previously reported procedure with several modifications [8]. Solid reagents (all Alfa Aesar) were used as received and included iron(II) chloride (99.5%) and tetrahydrate (98%), cobalt(II) chloride (99.7%) and hexahydrate (98%), nickel(II)

* Corresponding author. Fax: +1 5307528995.
E-mail address: kkovnir@ucdavis.edu (K. Kovnir).

http://dx.doi.org/10.1016/j.jssc.2015.09.016
0022-4596/© 2015 Elsevier Inc. All rights reserved.

chloride (99%) and hexahydrate (98%), and ammonium chloride (>99.5%). Formic acid (Acros Organics, 99%) and ethanol (Koptec, >99.5%) were also used as received. All operations involving samples prepared from anhydrous metal chlorides were performed under inert atmosphere in an argon-filled glovebox, while samples prepared from hydrated metal chlorides were treated under ambient atmosphere. Solvothermal syntheses were performed in 45-mL polytetrafluoroethylene (PTFE)-lined stainless steel acid digestion vessels (Parr Instrument Company), in which 2 mmol of anhydrous MCl_2 or hydrated $MCl_2 \cdot nH_2O$ (M=Fe, Co, Ni), 250 mg (4.67 mmol) NH_4Cl, 7.5 mL (0.2 mol) HCOOH, and 22.5 mL ethanol were mixed to achieve a filling fraction of 67%. The vessels were sealed tightly and the reaction was carried out in a programmable drying oven; the temperature was held at 150 °C for 4 hours, followed by cooling to 50 °C at a rate of 1 °C/h, at which point the oven was turned off and allowed to come to room temperature. Ambient-pressure syntheses were performed by adding 1 mmol MCl_2 or $MCl_2 \cdot nH_2O$ and 250 mg NH_4Cl to 10 mL HCOOH in a 20-mL scintillation vial; a hot-plate was used to heat the solution to the boiling point for ~15 min, followed by natural cooling with the hot plate turned off. Solid products were washed with ethanol and collected by vacuum filtration, with solvothermal reactions yielding large needle-like single crystals (Fig. 1B) and ambient-pressure reactions yielding mixtures of very fine needles and polycrystalline powders (Fig. 1A). The phase purity of each compound was confirmed with laboratory powder X-ray diffraction (PXRD) using a Rigaku MiniFlex 600 diffractometer with Cu-Kα radiation (Fig. 1C).

2.2. Characterization

Single-crystal X-ray diffraction datasets were collected for $NH_4MCl_2(HCOO)$ (M=Co, Ni) at 90 K using a Bruker Apex II diffractometer with graphite-monochromated Mo-Kα (λ=0.71037 Å) radiation. Two-component non-merohedral twinning was observed in both compounds; the components were separated manually in a reciprocal lattice viewer (RLATT in APEX2) [9], and each component could be indexed to the same C-centered monoclinic unit cell with different orientation matrices.

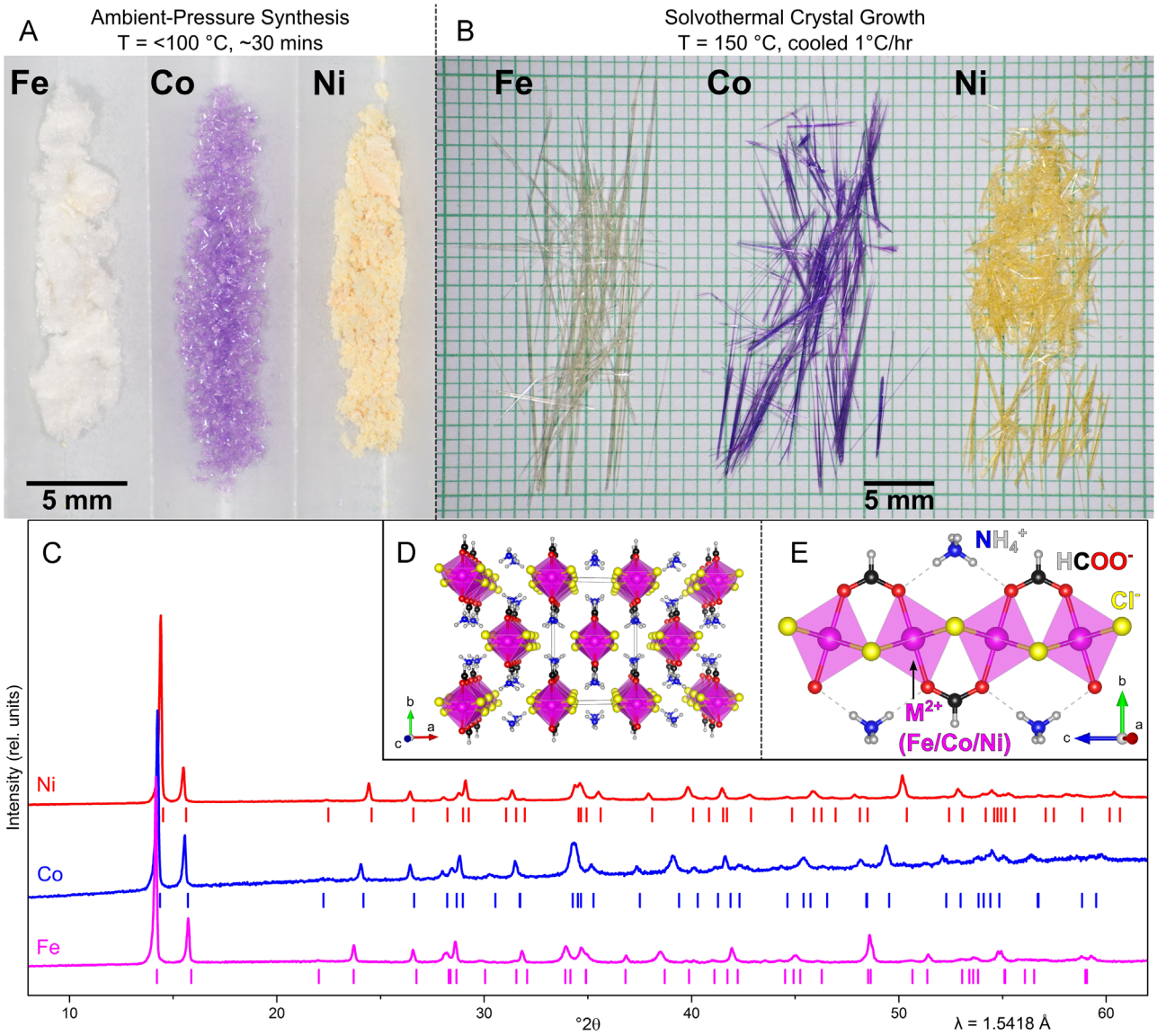

Fig. 1. A: Polycrystalline powders and B: single crystals of $NH_4MCl_2(HCOO)$ (M=Fe, Co, Ni), produced from ambient-pressure synthesis and solvothermal recrystallization, respectively. C: Room-temperature PXRD patterns for each compound, with calculated peak positions (>1% total intensity) indicated by tick marks below the patterns. Fe: magenta; Co: blue; Ni: red. D: General view of the crystal structure and E: one linear chain. M(Fe/Co/Ni): magenta; Cl: yellow; O: red; N: blue; C: black; H: white. (For interpretation of the references to color in this figure legend, the reader is referred to the web version of this article.)

Table 1
Single crystal data collection and structure refinement parameters for $NH_4MCl_2(HCOO)$ (M=Co, Ni)[a].

	$NH_4CoCl_2(HCOO)$	$NH_4NiCl_2(HCOO)$
Space Group	*C*2/*c* (no. 15)	
Temp. (K)	90 (2)	
λ (Å)	0.71073 (Mo Kα)	
a (Å)	7.730(2)	7.598(2)
b (Å)	11.269(2)	11.336(2)
c (Å)	6.844(1)	6.753(1)
β (deg)	107.90(3)	107.68(3)
V (Å)	567.3(2)	554.2(2)
Z	4	
ρ (g cm^{-3})	2.26	2.31
μ (mm^{-1})	3.85	4.35
θ (deg)	$3.07 < \theta < 30.53$	$3.34 < \theta < 32.04$
data/param.	875/45	941/45
R_1/wR_2	0.014/0.033	0.016/0.039
goodness-of-fit	1.10	1.11

[a] Further details are available from the Cambridge Crystallographic Data Centre by quoting the depository numbers CCDC 1412668 and 1412669.

Integration was performed with the Bruker SAINT software package [10], refining both twin components but constraining them to share the same unit cell. Multi-scan absorption correction was performed with TWINABS [11], in which Friedel opposites were merged. Both compounds were solved using only the main twin component in space group *C*2/*c* (no. 15) using the SHELX suite of programs [12], and final refinements were performed with anisotropic atomic displacement parameters for all non-hydrogen atoms and isotropic displacement parameters for hydrogen atoms. Further details about the data collection, structure refinement, and unit cell parameters are summarized in Table 1.

The magnetic structure of $NH_4FeCl_2(HCOO)$ was determined from low-temperature neutron diffraction data collected on beamline HB-2A at the High Flux Isotope Reactor (HFIR) at Oak Ridge National Laboratory (ORNL). Patterns were collected on a powder sample in a vanadium sample can using two wavelengths (Ge_{115}, $\lambda = 1.53618$ Å and Ge_{113}, $\lambda = 2.40608$ Å) at both 4 K and 15 K, with additional magnetic peaks appearing in the 4 K patterns.

The magnetic reflections have been indexed by using the "K-search" program (part of the Fullprof Suite package [13]) and revealed a commensurate antiferromagnetic magnetic structure with propagation vector **k**=(1,0,0) or (0,1,0). This implies the Fe atoms related by the C-centering operation have their moments inverted. Symmetry-allowed magnetic models, assuming **k**=(1,0,0) and the crystal space group *C* 2/*c*, have been generated using the SARAh Representational Analysis program [14] and MAXMAGN on the Bilbao Crystallographic Server [15]. There are two possible (symmetry-allowed) magnetic configurations where the magnetic moments at the two equivalent Fe positions ((0,0,0) and (0,0,0.5)) are related as follows: (μ_a, μ_b, μ_c), ($-\mu_a$, μ_b, $-\mu_c$) or (μ_a, μ_b, μ_c), (μ_a, $-\mu_b$, μ_c). The latter model corresponds to the magnetic space group P_C2_1/c (#14.84) and provided the best fit for our data.

Rietveld refinement was performed using the Fullprof Suite program on combined mode using the two aforementioned data sets (two neutron wavelengths) at each temperature. The nuclear structure was fully refined with isotropic atomic displacement parameters, and a magnetic phase was added to the 4 K refinement to account for the additional magnetic diffraction peaks. The μ_a and μ_c components of the magnetic moment were refined for the magnetic phase with propagation vector **k**=(1 0 0).

The magnetic properties of $NH_4MCl_2(HCOO)$ (M=Co, Ni) were measured with a Quantum Design MPMS-XL SQUID magnetometer, with temperature-dependent magnetic susceptibility collected from 2 to 300 K in an applied field of 0.01 T and isothermal magnetization collected in an applied field of 0.01–7 T at 2 K. Measurements were performed on powder samples held in gelatin capsules.

^{57}Fe Mössbauer spectra were collected at room temperature and 5 K for a powder sample of $NH_4FeCl_2(HCOO)$, which was mixed with hexagonal boron nitride to reduce preferred orientation and texturing effects. Spectra were collected using a conventional constant-acceleration spectrometer equipped with a ^{57}Co/Rh source held at room temperature, and least-squares fitting of the data was performed using the Recoil software package [16]. Centroid shifts (δ) are given with respect to metallic α-Fe at room temperature.

3. Results and discussion

3.1. Synthesis

Following our previous work with $NH_4FeCl_2(HCOO)$ [8], we attempted to expand our solvothermal and ambient-pressure synthetic methods to other 3*d* transition metals in the 2+ oxidation state, as changing the transition metal may lead to differing magnetic properties. Beginning with hydrated forms of the metal chlorides, it was found that the relative solubility of the desired product was highly dependent on both the identity of the transition metal and the exact quantity of water present in the reaction mixture. The target compounds are extremely soluble in water, but only sparingly soluble in mixtures of ethanol and formic acid; as has been shown for the iron compound, the amount of water introduced by the tetrahydrate starting material is insufficient to prevent the formation of $NH_4FeCl_2(HCOO)$, which precipitates out of the mixture shortly after the reagents are mixed. This reaction is also accelerated by heating the mixture to the boiling point, most likely due to the increased solubility of NH_4Cl in ethanol at elevated temperatures. In the case of the nickel compound, the use of a hexahydrate starting material does not appear to negatively affect the reaction, as the target compound immediately precipitates out of the solution as a fine yellow powder, and heating this mixture to boiling does not appear to solubilize a significant quantity of the solid product. However, the same is not true for the cobalt compound, which appears to be much more soluble than either the iron or nickel analogs. Upon mixing, the cobalt solutions take on the characteristic blue color, but remain clear even after heating to boiling and cooling to room temperature; only upon evaporation of the solvent do crystals of $NH_4CoCl_2(HCOO)$ form, along with crystals of $CoCl_2 \cdot nH_2O$ (n=2 or 6, depending on ambient humidity and duration of exposure). Similar results were obtained for solvothermal reactions starting from hydrated metal chlorides, though it was possible to obtain medium-sized single crystals of the nickel compound by increasing the reaction temperature to 200 °C.

It was observed that polycrystalline samples would hydrolyze after brief exposure to ambient atmosphere, especially for the cobalt compound, reforming the hydrated starting materials. In order to avoid this decomposition, the syntheses were modified in such a way that they could be performed in an argon-filled glovebox. The re-optimization of the reaction conditions for anhydrous starting materials revealed that the best yield of polycrystalline samples from ambient-pressure reactions could be obtained using pure formic acid as the solvent, and very large single crystals could be grown from solvothermal reactions using the same mixture of ethanol and formic acid as was reported previously for the Fe-containing compound (Fig. 1). The ambient-pressure reactions proceeded in a very similar fashion to those performed using hydrated metal chlorides, except in the case of the cobalt compound; while solvent evaporation was previously

necessary for crystallization, the use of anhydrous $CoCl_2$ allowed the target phase to crystallize with minimal solvent loss after 15 min of boiling, producing a very large quantity of 0.1–0.5 mm purple needles upon cooling. The solvothermal reactions cannot be performed using pure formic acid as the solvent, as even 10 mL in a 45-mL autoclave at 150 °C can build enough pressure to burst through two heavy-gauge steel rupture discs. However, simply switching to anhydrous metal chlorides and keeping the ethanol/formic acid concentrations constant, much larger and higher quality single crystals can be grown in a relatively short period of time. It was determined that if the reaction temperature was high enough to completely dissolve the solid products, then the size and quality of the resulting crystals were controlled only by the rate of cooling, with slower cooling producing larger and clearer crystals. 150 °C was sufficient for both the iron and cobalt compounds, as no polycrystalline powders remained under these reaction conditions, but a small amount was still present for the nickel compound, indicating that higher temperatures may be necessary to fully dissolve the products.

3.2. Magnetic structure of $NH_4FeCl_2(HCOO)$

We have already reported the synthesis, structure, and magnetic properties of $NH_4FeCl_2(HCOO)$, which appeared to be an antiferromagnet ($T_N = 6$ K) with complex non-collinear ordering of the magnetic moments based on a combination of data obtained from SQUID magnetometry and ^{57}Fe Mössbauer spectroscopy [8]. However, we were not previously able to determine the true magnetic structure, and there was an indication of a possible low-temperature structural transition in the Mössbauer data. Our previous Mössbauer experiment was performed on an assembly of crystals oriented with the crystallographic *c*-axis perpendicular to the incoming gamma radiation, and there was also a small admixture of a magnetic iron oxide impurity. In order to rule out the effects of the intentional preferred orientation, or possible contribution from the magnetic impurity, the measurement was repeated on a powder sample produced by ambient-pressure synthesis, which was mixed with hexagonal boron nitride to further reduce preferred orientation. Spectra were collected at room temperature and at 5 K (Fig. 2). The room temperature spectrum showed no evidence of any iron oxide impurities, and was well fit by a single component with $\delta = 1.146$ mm/s and an electric quadrupole splitting (ΔE_Q) of 2.587 mm/s. This is in excellent agreement with our previous measurement, despite the difference in sample preparation. The magnetically-split 5 K spectrum was also very similar to what we have already reported. As before, the positions and intensities of the peaks indicate that the spectrum is a result of mixed hyperfine interactions, due to the large Electric Field Gradient (EFG) causing quadrupole splitting of a similar magnitude to the magnetic hyperfine interaction. Further details of this fitting model can be found in our previous report. In the present work all of our attempts to fit the 5 K spectrum with a single component did not yield satisfactory results (Fig. 2B); a two-component model was necessary to achieve a good fit (Fig. 2C), again indicating that at 5 K iron atoms occupy two crystallographically inequivalent positions within the structure. Table 2

To assess the possibility of a structural distortion at low temperature and determine the absolute magnetic structure, neutron powder diffraction patterns were collected at 15 K and 4 K, respectively above and below the Néel temperature. All of the peaks present in the 15 K pattern were well described by the structural model derived from the 90 K single crystal X-ray diffraction experiment, and the only significant difference in the 4 K pattern was the appearance of magnetic peaks (Fig. 3A); this indicates that there was no structural phase transition or distortion of the average structure at low temperature, though this does not preclude the possibility of a local distortion that could give rise to the two distinct Mössbauer components, which would not be visible by neutron diffraction.

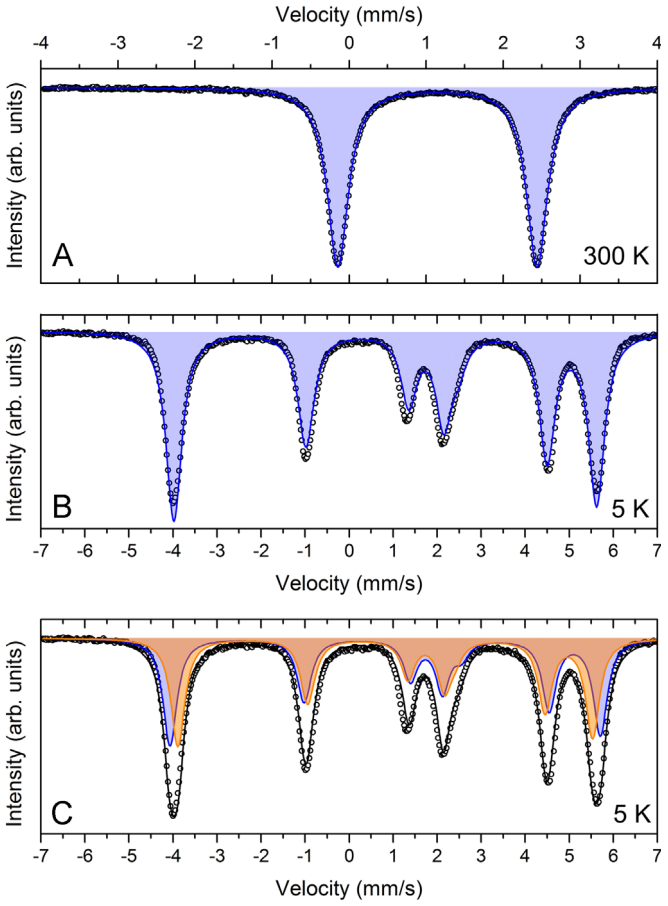

Fig. 2. A: Room-temperature and B: 5 K Mössbauer spectra with single-component fits for $NH_4FeCl_2(HCOO)$. C: Two-component fitting of the 5 K spectrum. Experimental data: black circles; calculated spectrum: black line; component spectra: blue and orange lines.

Table 2
Summary of refined Mössbauer parameters for 300 K and 5 K spectra.

Temperature	300 K	5 K		
Parameter	A	B	C	
	Q_1	Q_1	Q_1	Q_2
δ (mm/s)	1.146(1)	1.288(1)	1.290(1)	1.288(1)
B_{hf} (T)	–	26.3(1)	26.5(1)	26.2(1)
ΔE_Q (mm/s)	2.587(1)	–	–	–
$e^2qQ/2$ (mm/s)	–	2.710(2)	2.837(3)	2.545(3)
η	–	0.734(2)	0.752(2)	0.686(2)
Γ (mm/s)	0.33(1)	0.44(1)	0.38(1)	0.38(1)
ϕ_{Hq} (deg)	–	44.4(1)	43.9(4)	44.9(4)
θ_{Hq} (deg)	–	90.0(2)	90.0(3)	90.4(4)
I (%)	100	100	50(2)	50(2)

Modeling of the centroid shift (δ), magnetic hyperfine field (B_{hf}), EFG interaction ($e^2qQ/2$) and asymmetry (η) parameters, linewidth (Γ), azimuthal (ϕ_{Hq}) and polar (θ_{Hq}) angles of B_{hf} with respect to the principal coordinate axes of the EFG, and intensity (I) are based on a full static Hamiltonian analysis [17,18].

The additional magnetic peaks could be described with the propagation vector $\mathbf{k} = (1\,0\,0)$ (Fig. 3B) and magnetic moments arranged in a ferromagnetic fashion along the chains, with antiferromagnetic coupling between neighboring chains (Fig. 3C–F). This is the same set of interactions reported for $[(CH_3)_2NH_2][Fe(N_3)_2(HCOO)]$, a

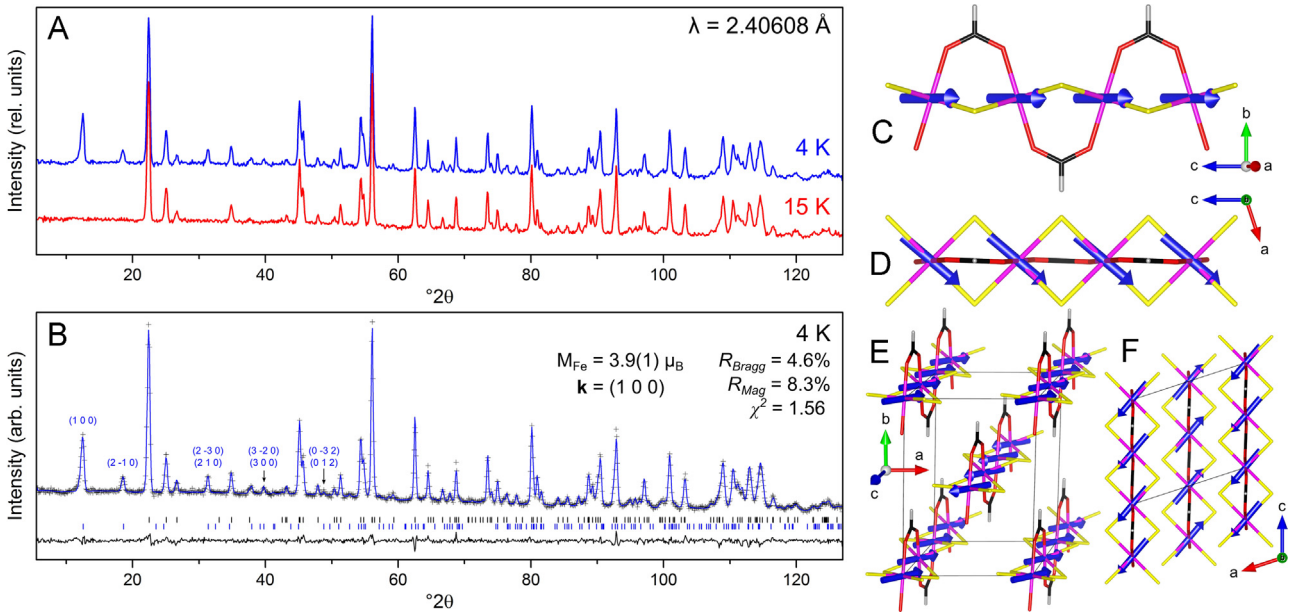

Fig. 3. A: Comparison of 15 K (red) and 4 K (blue) neutron powder diffraction patterns (λ=2.40608 Å) of $NH_4FeCl_2(HCOO)$, with the 4 K pattern exhibiting additional magnetic peaks. B: Rietveld refinement of the 4 K pattern. Tick marks show calculated peak positions for the nuclear (black) and magnetic (blue) phases. C–D: Side and top views of a linear chain, and E–F: two general views of the magnetic structure, with magnetic moments shown as blue arrows. NH_4^+ omitted for clarity. (For interpretation of the references to color in this figure legend, the reader is referred to the web version of this article.)

compound with a similar structure but with end-on azido ligands in place of the bridging chlorides and a bulkier dimethylammonium cation [19], although the longer intra-chain Fe–Fe distances in $NH_4FeCl_2(HCOO)$ lead to weaker exchange interactions and a lower ordering temperature. The refined magnetic moment of the iron atom is directed very nearly along the [1 0 −1] direction and has a magnitude of 3.9(1) μ_B, which is very close to the spin-only magnetic moment of 4 μ_B for high-spin (S=2) Fe^{2+}.

Although this magnetic structure differs significantly from the models we suggested in our previous report, it is actually in much better agreement with our oriented single-crystal magnetometry and Mössbauer data. The key stumbling point in our prior assignment of a magnetic model was the observation of a negative asymptotic Curie temperature (θ) for the powder sample; we had reasonably interpreted this as an indication of antiferromagnetic nearest-neighbor interactions, which ultimately precluded our consideration of the correct model. One potential cause for the negative θ is the presence of an iron oxide admixture, which had been observed by Mössbauer spectroscopy; another possibility is that the dominant interactions were in fact antiferromagnetic inter-chain interactions, rather than nearest-neighbor interactions. Nevertheless, our previous magnetic studies of an oriented single crystal had shown a positive θ when the magnetic field was oriented parallel to the crystallographic c-axis, corresponding to the ferromagnetic coupling in the direction of chain propagation. The present Mössbauer fitting indicated that the magnetic moments were directed ~90° from the z-axis and ~45° from the y-axis of the EFG; our assumption that the short Fe–O bond comprised the z-axis of the EFG was correct, though it appears that the y-component of the EFG was not along one of the Fe–Cl bonds, but instead directed along the chains. Taking both of these pieces of information into account, the moments should be coupled ferromagnetically within the chains and directed towards one of the chloride ligands, in perfect agreement with the magnetic structure determined from low temperature neutron diffraction. The ferromagnetic coupling is likely mediated by 90° super-exchange through the bridging chloride ligands, as this type of magnetic interaction is relatively common in metal chlorides [20] and has been reported for a variety of compounds with similar 1D chain structures [19,21,22].

3.3. Structure comparison of $NH_4MCl_2(HCOO)$ (M=Fe, Co, Ni)

While all three compounds are isostructural, the relative decrease in the size of the transition metal cation from Fe^{2+} to Co^{2+} to Ni^{2+} led to subtle changes in the structure that may play an important role in determining the magnetic properties. As can be seen in Fig. 4A, decreasing the size of the metal cation caused the a, c, and β parameters to decrease, while the b parameter was observed to increase. Interestingly, the magnitudes of these changes are such that the shortest inter-chain M–M distance, which corresponds to the shortest antiferromagnetic interaction in the magnetic structure of $NH_4FeCl_2(HCOO)$, varies by less than 0.01 Å. The relative invariance of this distance is made more unusual by the fact that the individual chains also decrease in both length and volume with the size of the transition metal cation; as shown in Fig. 4B–C, the shorter M–Cl bonds decrease the intra-chain M–M distance and the overall length of the chain, while the shorter M–O bonds serve to decrease the volume of the chains, effectively widening the gaps between chains along the b-direction. Reducing the size of the metal cation also led to a small narrowing of the chains in the a-direction and straightening along the c-direction, due to decreased internal Cl–M–Cl angles and less severe tilt angles between adjacent MCl_4 planes. While these changes slightly increase the relative length of the chains in the c-direction, the effects are minimal compared to the overall reduction in chain length imparted by the shortened M–Cl and M–O bonds.

3.4. Magnetic properties

It is intriguing to compare the magnetic properties of $NH_4MCl_2(HCOO)$ (M=Fe, Co, Ni) considering that their inter-chain M–M distances are equal, but the intra-chain M–M distance is significantly reduced for the cobalt and nickel analogs. We have previously reported the detailed magnetic characterization of $NH_4FeCl_2(HCOO)$ [8]; the data from the powder sample is reproduced here to facilitate a comparison with the newly reported

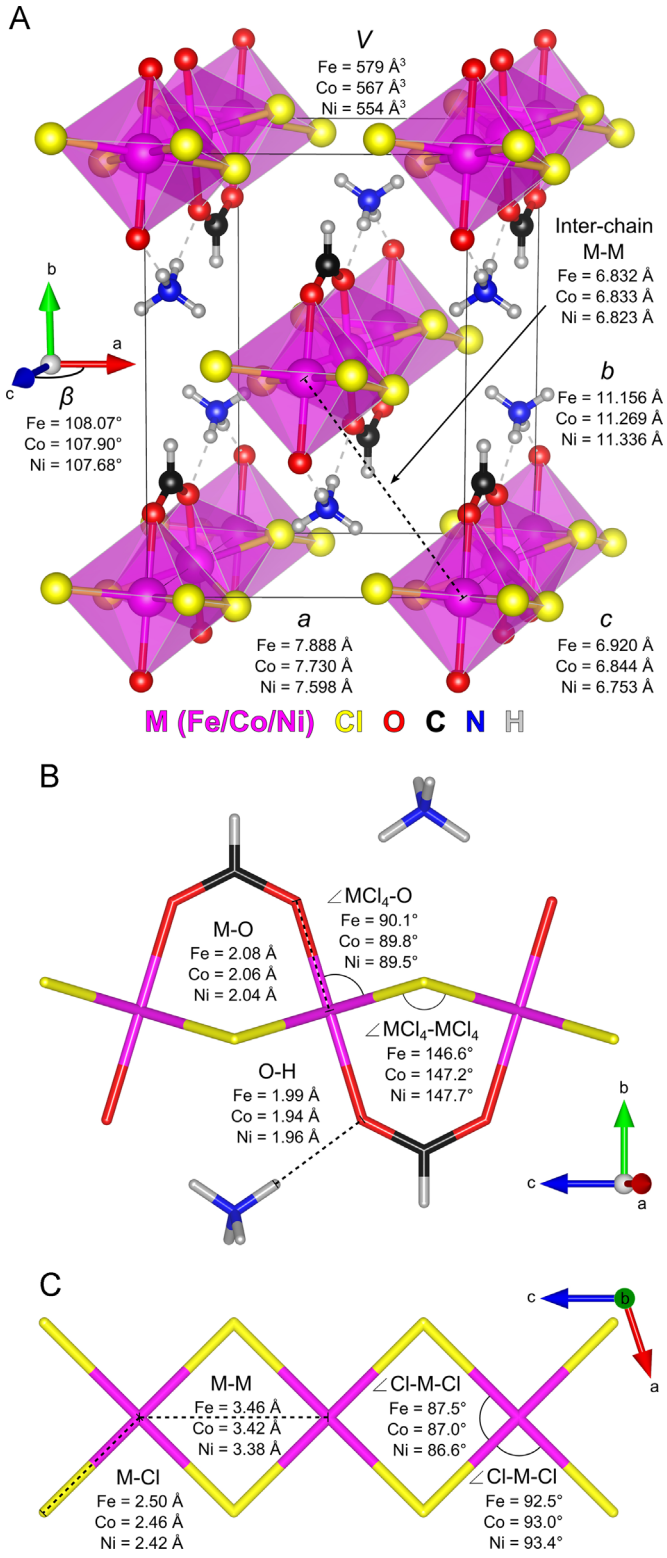

Fig. 4. A: One unit cell of $NH_4MCl_2(HCOO)$ (M=Fe*, Co, Ni) with labels comparing the lattice parameters of all three compounds. B: Side view of a linear chain. C: Top view of a linear chain with NH_4^+ and $HCOO^-$ omitted for clarity. M (Fe/Co/Ni): magenta; Cl: yellow; O: red; N: blue; C: black; H: white. *Data for $NH_4FeCl_2(HCOO)$ are from our previous report [8], and are shown for ease of comparison. (For interpretation of the references to color in this figure legend, the reader is referred to the web version of this article.)

compounds.

As can be seen in Fig. 5, $NH_4NiCl_2(HCOO)$ behaves similarly to the iron-containing compound, exhibiting the characteristic peak of

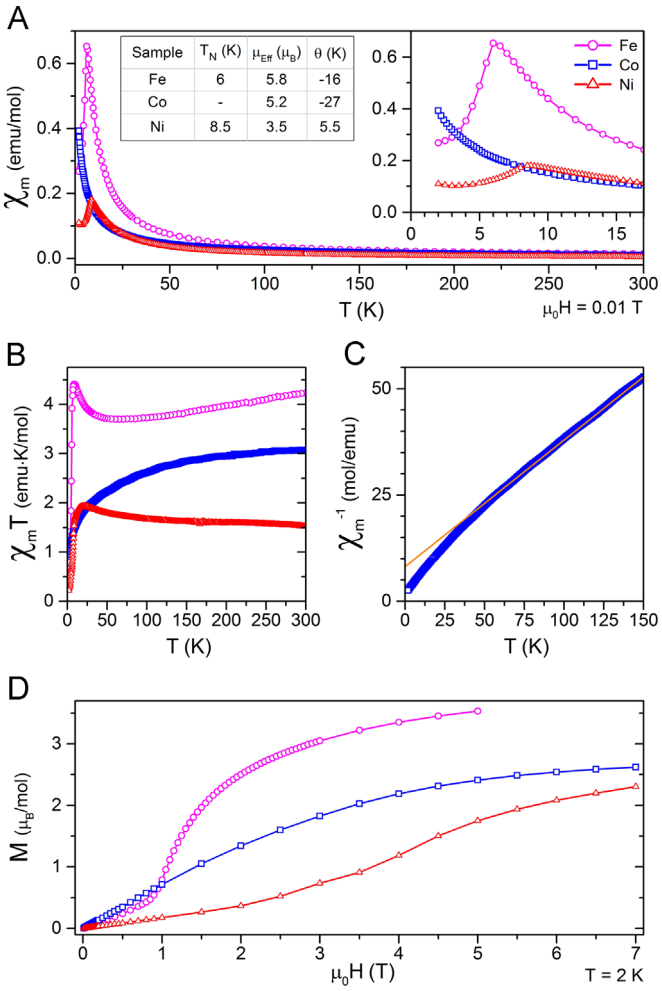

Fig. 5. A: Temperature-dependent magnetic susceptibility of $NH_4MCl_2(HCOO)$ (M=Fe*, Co, Ni). Insets: Curie–Weiss fit parameters of high-temperature data and an expanded view of the low-temperature region. B: $\chi_m T$ product plot for each compound. C: Inverse magnetic susceptibility for $NH_4CoCl_2(HCOO)$ showing downward deviation from Curie–Weiss behavior at low temperature. D: Isothermal magnetization for each compound. Fe: magenta circles; Co: blue squares; Ni: red triangles. *Data for $NH_4FeCl_2(HCOO)$ are from our previous report [8], and are shown for ease of comparison. (For interpretation of the references to color in this figure legend, the reader is referred to the web version of this article.)

antiferromagnetic ordering at 8.5 K. Furthermore, $NH_4NiCl_2(HCOO)$ also exhibits a broad metamagnetic transition between 2 T and 5 T (Fig. 5D), though it is much broader than the one observed in the iron analog and occurs at a higher field strength. This relatively unusual form of magnetic transition has been reported for a number of similar one-dimensional chain structures [19,22], all of which are characterized by ferromagnetic intra-chain interactions and weaker antiferromagnetic inter-chain interactions; in these materials an applied magnetic field will initially cause only a slight canting of the moments, but a sufficiently high field will overcome the antiferromagnetic coupling between chains and induce three-dimensional ferromagnetic ordering, giving rise to a metamagnetic transition. The highest applied magnetic field of 7 T was not sufficient to fully saturate the magnetization, but the 7 T value of 2.4 μ_B/mol exceeds the expected spin-only moment for Ni^{2+} (2 μ_B/mol); furthermore, Curie–Weiss fitting of the high-temperature data gives an effective magnetic moment (μ_{Eff}) of 3.5 μ_B, also surpassing the expected spin-only value of 2.83 μ_B. These unusually high values cannot be explained by a contribution from orbital angular momentum, as the octahedral coordination environment of the Ni^{2+} ion is strongly distorted to an approximate D_{4h} symmetry with a

non-degenerate electronic ground state; additional measurements of oriented single crystal samples or neutron diffraction studies will be necessary to clarify the source of the additional moment. The nickel compound also exhibits stronger antiferromagnetic coupling than the iron compound, as evidenced by the higher Néel temperature and magnetic field required for the metamagnetic transition (Fig. 5A,D). Curie–Weiss fitting yields a θ of 5.5 K, indicating that the nearest-neighbor interactions are ferromagnetic, which would be expected if the nickel compound had a similar magnetic structure to the iron compound and the intra-chain coupling was strong enough to be the dominant interaction at high temperature. The increased strength of the magnetic coupling is likely caused by the decreased intra-chain M–M distance in the nickel compound relative to the iron analog (Fig. 4C), as closer contacts between magnetic atoms are known to improve magnetic exchange [23].

The cobalt analog is perhaps more interesting, in that it has a completely different behavior than the iron or nickel compounds. In terms of the crystal structure and magnetic moment, it should have intermediate properties, but as can be seen in Fig. 5A the cobalt compound does not undergo any 3D magnetic ordering above 2 K. Interestingly, it does not behave as a simple paramagnet either; Curie–Weiss fitting of the high temperature portion of the inverse susceptibility shows a downward deviation at low temperature (Fig. 5C), typical for some sort of ferro- or ferrimagnetic interactions, yet the strongly negative θ (–27 K) is indicative of dominant antiferromagnetic nearest-neighbor interactions. χ_mT also shows a continuous downward trend with decreasing temperature beginning as high as 250 K (Fig. 5B), further supporting the case for dominant antiferromagnetic interactions. As the powder sample of the iron compound also exhibited a negative θ when it in fact had ferromagnetic nearest-neighbor interactions, we cannot be sure that the cobalt compound is characterized by antiferromagnetic intra-chain coupling without additional experimental confirmation. We can, however, safely conclude that the magnetic structure is unlike those of the iron and nickel analogs. One possible reason for this could be strong spin–orbit coupling, which is known to occur for high-spin Co^{2+} ions in other compounds [24] and could lead to a significantly different orientation of the magnetic moments within the chains. Magnetic measurements of oriented single crystals or low-temperature neutron diffraction will be necessary to develop a complete picture of the magnetic coupling in this compound.

4. Conclusion

We have successfully expanded the $NH_4MCl_2(HCOO)$ family of compounds to include cobalt and nickel in addition to iron, and with slight modifications to our earlier synthetic procedures we have developed a simple set of reaction conditions suitable for producing either polycrystalline powders via an ambient-pressure route or large, high-quality single crystals with the use of a solvothermal technique. The exclusion of water from the system is beneficial to the formation of the desired product, and in the case of iron the exclusion of oxygen prevents the formation of iron oxides that have previously complicated the measurement of its magnetic properties. We have now determined the magnetic structure of $NH_4FeCl_2(HCOO)$ via low-temperature neutron diffraction experiments, which is characterized by ferromagnetic intra-chain interactions and antiferromagnetic inter-chain coupling. The cobalt and nickel analogs were determined to be isostructural with $NH_4FeCl_2(HCOO)$; while decreasing the size of the M^{2+} cation led to shorter intra-chain M–M distances and an overall contraction of the lattice parameters, there was an unusual expansion of the *b* parameter that allowed the inter-chain M–M distance to remain invariant for all three compounds. Magnetic measurements showed that the nickel analog behaves similarly to the iron compound, though the decreased M–M separation leads to stronger magnetic coupling and a higher Néel temperature. In contrast, the cobalt analog appeared to have dominant antiferromagnetic interactions but did not exhibit any 3D magnetic ordering above 2 K. As these three isostructural compounds exhibited significantly different magnetic properties, all of which are likely to be anisotropic, it would be intriguing to expand the $NH_4MCl_2(HCOO)$ family of compounds to other transition metals; further studies of these and related compounds are currently underway.

Acknowledgments

The University of California, Davis is gratefully acknowledged for financial support. The work at the Oak Ridge National Laboratory was sponsored by the Scientific User Facilities Division, Office of Basic Energy Sciences, U.S. Department of Energy (DOE).

Appendix A. Supplementary material

Supplementary data associated with this article can be found in the online version at http://dx.doi.org/10.1016/j.jssc.2015.09.016.

References

[1] A. Rabenau, The role of hydrothermal synthesis in preparative chemistry, Angew. Chem.-Int. Edit. Engl. 24 (1985) 1026–1040, http://dx.doi.org/10.1002/anie.198510261.
[2] M. Viertelhaus, P. Adler, R. Clerac, C.E. Anson, A.K. Powell, Iron(II) formate $[Fe(O_2CH)_2]\cdot 1/3HCO_2H$: a mesoporous magnet-solvothermal syntheses and crystal structures of the isomorphous framework metal(II) formates $[M(O_2CH)_2]$-*n*(Solvent) (M=Fe, Co, Ni, Zn, Mg), Eur. J. Inorg. Chem. 4 (2005) 692–703, http://dx.doi.org/10.1002/ejic.200400395.
[3] Z.M. Wang, K.L. Hu, S. Gao, H. Kobayashi, Formate-based magnetic metal-organic frameworks templated by protonated amines, Adv. Mater. 22 (13) (2010) 1526–1533, http://dx.doi.org/10.1002/adma.200904438.
[4] B. Li, X. Zhang, J. Tian, J. Zhang, The magneto-structural correlation of two novel 1D antiferromagnetic chains with different magnetic behaviors, Polyhedron 30 (2011) 3100–3105, http://dx.doi.org/10.1016/j.poly.2011.02.045.
[5] X.-Y. Wang, Z.-M. Wang, S. Gao, Constructing magnetic molecular solids by employing three-atom ligands as bridges, Chem. Commun. 3 (2008) 281–294.
[6] A.V. Palii, O.S. Reu, S.M. Ostrovsky, S.I. Klokishner, B.S. Tsukerblat, Z.-M. Sun, J.-G. Mao, A.V. Prosvirin, H.-H. Zhao, K.R. Dunbar, A highly anisotropic cobalt(II)-based single-chain magnet: exploration of spin canting in an antiferromagnetic array, J. Am. Chem. Soc. 130 (2008) 14729–14738, http://dx.doi.org/10.1021/ja8050052.
[7] G.C. Xu, W. Zhang, X.M. Ma, Y.H. Chen, L. Zhang, H.L. Cai, Z.M. Wang, R. G. Xiong, S. Gao, Coexistence of magnetic and electric orderings in the metal-formate frameworks of NH_4 $M(HCOO)_3$, J. Am. Chem. Soc. 133 (2011) 14948–14951, http://dx.doi.org/10.1021/ja206891q.
[8] J.T. Greenfield, S. Kamali, N. Izquierdo, M. Chen, K. Kovnir, $NH_4FeCl_2(HCOO)$: synthesis, structure, and magnetism of a novel low-dimensional magnetic material, Inorg. Chem. 53 (2014) 3162–3169, http://dx.doi.org/10.1021/ic403173v.
[9] Bruker, RLATT in APEX2. Version 2014.11-0, Bruker AXS Inc., Madison, Wisconsin, USA, 2014.
[10] Bruker, SAINT. Version 8.30A, Bruker AXS Inc., Madison, Wisconsin, USA, 2012.
[11] Bruker, TWINABS. Version 2008/1, Bruker AXS Inc., Madison, Wisconsin, USA, 2008.
[12] G.M. Sheldrick, A short history of SHELX, Acta Crystallogr. A64 (2008) 112–122, http://dx.doi.org/10.1107/s0108767307043930.
[13] J. Rodriguez-Carvajal, Recent advances in magnetic structure determination by neutron powder diffraction, Physica B 192 (1993) 55–69, http://dx.doi.org/10.1016/0921-4526(93)90108-I.
[14] A.S. Wills, A new protocol for the determination of magnetic structures using simulated annealing and representational analysis (SARAh), Physica B 276 (2000) 680–681, http://dx.doi.org/10.1016/S0921-4526(99)01722-6.
[15] J.M. Perez-Mato, S.V. Gallego, E.S. Tasci, L. Elcoro, G. de la Flor, M.I. Aroyo, Symmetry-Based Computational Tools for Magnetic Crystallography, Annu. Rev. Mater. Res. 45 (2015) 217–248, http://dx.doi.org/10.1146/annurev-matsci-070214-021008.
[16] K. Lagarec, D.G. Rancourt, Recoil, Mössbauer Spectral Analysis Software for Windows, Version 1.0, 1998.

[17] P. Gütlich, in: U. Gonser (Ed.), Mössbauer Spectroscopy, vol. 5, Springer, Berlin, Heidelberg, 1975, pp. 53–96, http://dx.doi.org/10.1007/3540071202_14.
[18] N. Blaes, H. Fischer, U. Gonser, Analytical expression for the Mössbauer lineshape of ^{57}Fe in the presence of mixed hyperfine interactions, Nucl. Instrum. Methods Phys. Res., Sect. B 9 (1985) 201–208, http://dx.doi.org/10.1016/0168-583x(85)90683-4.
[19] T. Liu, Y.J. Zhang, Z.M. Wang, S. Gao, Two chain compounds of $[M(N_3)_2(HCOO)][(CH_3)_2NH_2]$ (M=Fe and Co) with a mixed azido/formato bridge displaying metamagnetic behavior, Inorg. Chem. 45 (2006) 2782–2784, http://dx.doi.org/10.1021/ic0521527.
[20] A.F. Orchard, Magnetochemistry, Chapter 3, Oxford University Press Inc., New York, 2003, ISBN: 978-0198792789.
[21] J.D. Martin, R.F. Hess, P.D. Boyle, Synthesis of $[NH_4]MnCl_2(OAc)$ and $[NH_4]_2MnCl_4(H_2O)_2$ by solvothermal dehydration and structure/property correlations in a one-dimensional antiferromagnet, Inorg. Chem. 43 (2004) 3242–3247, http://dx.doi.org/10.1021/ic049881r.
[22] Y.-Q. Wen, Y. Ma, Y.-Q. Wang, X.-M. Zhang, E.-Q. Gao, Cobalt(II) metamagnet built from ferromagnetic chains with mixed bis(azido)(carboxylate) bridges, Inorg. Chem. Commun. 20 (2012) 46–49, http://dx.doi.org/10.1016/j.inoche.2012.02.011.
[23] K.H.J. Buschow, F.R. de Boer, Physics of Magnetism and Magnetic Materials, Kluwer Academic Publishers, New York (2003) http://dx.doi.org/10.1007/b100503, Chapter 4.
[24] R.L. Carlin, Magnetochemistry, Springer-Verlag, New York (1986) http://dx.doi.org/10.1007/978-3-642-70733-9, Chapter 4.